Eur. Phys. J. A **27**, 313–320 (2006)
DOI 10.1140/epja/i2004-10309-0

THE EUROPEAN PHYSICAL JOURNAL A

Low-lying magnetic dipole strength distribution in the γ-soft even-even $^{130-136}$Ba

E. Guliyev[1,2,a], F. Ertuğral[1], and A.A. Kuliev[1]

[1] Physics Department, Faculty of Arts and Sciences, Sakarya University, 54100 Serdivan, Adapazari, Turkey
[2] Institute of Physics, Academy of Sciences, H. Cavid Avenue 33, Baku, Azerbaijan

Received: 10 October 2004 / Revised version: 4 April 2006 /
Published online: 2 May 2006 –
Communicated by G. Orlandini

Abstract. In this study the scissors mode 1^+ states are systematically investigated within the rotational invariant Quasiparticle Random Phase Approximation (QRPA) for $^{130-136}$Ba isotopes. We consider the 1^+ vibrations generated by the isovector spin-spin interactions and the isoscalar and isovector quadrupole-type separable forces restoring the broken symmetry by a deformed mean field according to A.A. Kuliev *et al.* (Int. J. Mod. Phys. E **9**, 249 (2000)). It has been shown that the restoration of the broken rotational symmetry of the Hamiltonian essentially decreases the $B(M1)$ value of the low-lying 1^+ states and increases the collectivization of the scissors mode excitations in the spectroscopic energy region. The agreement between the calculated mean excitation energies as well as the summed $B(M1)$ value of the scissors mode excitations and the available experimental data of ^{134}Ba and ^{136}Ba is rather good. A destructive interference between the orbit and spin part of the $M1$ strength has been found for barium isotopes near the shell closer. For all the nuclei under investigation, the low-lying $M1$ transitions have $\Delta K = 1$ character as it is the case for the well-deformed nuclei.

PACS. 21.10.Re Collective levels – 21.10.Hw Spin, parity, and isobaric spin – 21.60.Ev Collective models

1 Introduction

The existence of the low-lying orbital magnetic dipole scissors mode states is now well established as fundamental excitations in deformed nuclei [1]. The presence of states with orbital character has been firstly announced theoretically within the semi-classical two-rotor model [2] and the interacting boson model [3], with proton-neutron degrees of freedom. This mode was first observed in ^{156}Gd in high-resolution electron scattering experiments in 1984 [4]. Nowadays this mode has been found for isotopes with permanent deformation in the wide region beginning from the light nuclei (such as ^{46}Ti) up to the actinides also including the transitional and γ-soft nuclei (see refs. [1, 5] and references therein). The remarkable features of the scissors mode obtained from experimental results are the quadratic dependence of the summed $B(M1)$ values on the ground-state deformation parameter δ and the strong fragmentation of the $M1$ strength over the pairing gap energy up to 4 MeV excitation energy [6–9] concentrated around 3 MeV. This mode was first studied in schematic models [10–13]. After its experimental discovery, microscopic approaches were developed for a more detailed investigation of its properties [14–18]. Several studies have been devoted to the δ^2 law. This has been described with fair success within phenomenological models [19–22] as well as in microscopic approaches [23–28]. The microscopic calculations yield a strength more or less quadratic in the deformation parameter [23–28]. More recently, investigations using rotational invariant QRPA [27], the sum-rule approach [19] and the generalized coherent model [20] have shown that these models reproduce the excitation energy as well as the quadratic dependence of the summed $M1$ strength of the mode in heavy even-even deformed nuclei. For recent reviews on theoretical aspects of the scissors mode see refs. [29,30]. In most cases, particularly for strongly deformed rare-earth nuclei near mid-shell, the variations of the mean excitation energy and the total $M1$ excitation strength of the mode are small [8, 21]. However, while the global properties of the scissors mode are reasonably understood in regions of moderate to large deformations, the nature of the scissors mode is an open question in nuclei near shell closures where the simple geometrical picture of a scissors-like motion of deformed proton and neutron bodies breaks down. It would be desirable to confirm the features of the scissors mode in other γ-soft deformed nuclei. The dipole excitation strength distribution has been investigated experimentally in less-deformed transitional nuclei, *e.g.*, in the

[a] e-mail: aguliyev@cern.ch

γ-soft nuclei ^{194,196}Pt [31,32], ^{134,136}Ba [33,34], in transitional osmium nuclei [35], and in several vibrational nuclei of the tellurium isotopic chains [36,37] and ^{94}Mo [38]. In all of these cases the scissors mode was observed, however, with decay properties differing considerably from the findings in well-deformed rotors because of the loss of axial symmetry and the establishment of the d-parity quantum number [39]. Unfortunately, the scarcity of the data of transition nuclei does not allow the systematic analysis of the properties of the mode as a function of deformation parameters or of the mass number A. Available experimental data of two platinum and barium isotopes are not sufficient for a decisive conclusion for the scissors mode properties of transitional nuclei. It would be important to extend the (γ,γ') studies to γ-soft nuclei with improved sensitivity in order to firmly establish deviations from the δ-dependence in nuclei near shell closure $(N,Z)=82$. In view of this, the Ba isotopic chain with its stable even-even isotopes, with a considerable ground-state deformation [40–42], offers the rare possibility to study the scissors mode properties in nuclei of the $A=130$ mass region.

Theoretical investigations of the scissors mode for transitional nuclei, like Ba isotopes around $A=130$, are scant. By now, there have been several calculations [43–46] dealing with 1^+ excitations in a number of Ba nuclei, which were reported two decades ago. The predictive power of these calculations, however, is limited in general. In papers [44,45] IBA-2 has been previously applied to even-even $^{128-134}$Ba. The phenomenological IBA-2 predicts a single state below 4 MeV but QRPA, which uses a deformed single-particle basis, predicts two [46] with small $B(M1)$ values. Whereas the experimental $M1$ strength distributions in ^{134}Ba [33] up to 4 MeV exhibit much more fragmentation and *larger* amount of $B(M1)=0.56\mu_N^2$ (than predicted by the above-mentioned calculations).

Based on these observations and by applying a method developed in [27] for ^{130,132,134,136}Ba isotopes, the fragmentation of the scissors mode 1^+ states and the dependence of the $B(M1)$ transition strength on the deformation parameter have been investigated in this study. Although the underlying assumption of an axially deformed mean field may be questioned for the heavy barium nuclei, at present it represents the only possible approach to an improved understanding of the fine structure experimentally observed for the dipole modes [33,34]. The high density of the observed dipole states cannot be explained with the assumption that the nucleus is spherical in the ground state, and this is in fact confirmed by the previous calculations in QRPA [47,48] and the quasiparticle-phonon model [49]. The use of the method presented in [27] for this study is motivated by the satisfactory description of the experimental fragmentation and δ^2-dependence of the summed $B(M1)$ value of the scissors mode in Sm, Nd, Ce and Te isotopic chains on the basis of the rotationally invariant QRPA [27,28,50].

2 Theory

It is well known that the single-quasiparticle Hamiltonian of deformed nuclei is not invariant under rotational transformations. Therefore, the low-lying branch of $K^\pi=1^+$ excitations does not have vibrational nature, but rather is associated with rotational band of the ground state with energy $\omega_0=0$. Separating the spurious state with the energy $\omega_0=0$ from the vibrational ones is one of the fundamental requirements for the microscopic models. Various methods were elaborated for the separation of the spurious state from the vibrational ones [51–55]. A complete separation of the rotational mode from the vibrational ones has been achieved in the ref. [54] using the deformed mean field derived in Hartree approximation self-consistently from the separable rotational invariant quadrupole-quadrupole interaction in schematic RPA. For recent reviews on the theoretical aspects of the scissors mode, see [30]. A more practical method of restoring the broken symmetry by means of the isoscalar interactions in the QRPA for the separation of spurious states was suggested in ref. [52]. In the previous approaches and refs. [14, 56,57] the symmetry-restoring constraint was applied to the proton and neutron pieces of the Hamiltonian. Here we enforce such a constraint explicitly and separately on the isoscalar and isovector terms of the Hamiltonian. This enables us to disentangle the isoscalar from the isovector contributions. The generalization of the method for separation of the spurious rotational state with zero energy to a realistic case in which two different isoscalar and isovector restoring interactions in the Hamiltonian are present has been performed in [27].

Assuming that the isoscalar h_0 and isovector h_1 restoring interaction determined in [27] and the spin-spin forces produce the 1^+ states in deformed nuclei, the model Hamiltonian representing these states could be considered as

$$H=H_{sqp}+h_0+h_1+V_{\sigma\tau}. \tag{1}$$

Here, H_{sqp} is the Hamiltonian of the single-quasiparticle motion and $V_{\sigma\tau}$ takes into account the spin-isospin interaction of the form

$$V_{\sigma\tau}=\frac{1}{2}\chi_{\sigma\tau}\sum_{i\neq j}\vec{\sigma}_i\vec{\sigma}_j\vec{\tau}_i\vec{\tau}_j, \tag{2}$$

where, $\vec{\sigma}$ and $\vec{\tau}$ are the Pauli matrices that represent the spin angular-momentum operator and the isospin, respectively.

According to ref. [27] the rotational invariance of the single-quasiparticle Hamiltonian can be restored with the aid of a separable isoscalar and isovector effective interaction of the form

$$h_0=-\frac{1}{2\gamma_0}\sum_v\big[H_{sqp}-V_1,J_v\big]^+\big[H_{sqp}-V_1,J_v\big], \tag{3}$$

and

$$h_1=-\frac{1}{2\gamma_1}\sum_v\big[V_1(r),J_v\big]^+\big[V_1(r),J_v\big], \tag{4}$$

where

$$\gamma^{(v)} = \left[J_v^+, \left[H_{sqp}, J_v\right]\right]_{QRPA},$$
$$\gamma_1^{(v)} = \left[J_v^+, \left[V_1(r), J_v\right]\right]_{QRPA}, \quad (5)$$

and

$$\gamma^{(-1)} = \gamma^{(+1)} = \gamma,$$
$$\gamma_1^{(-1)} = \gamma_1^{(+1)} = \gamma_1,$$
$$\gamma_0 = \gamma - \gamma_1 \ \gamma_1 = \gamma_1^n - \gamma_1^p. \quad (6)$$

Here, the isoscalar γ_0 and isovector γ_1 coupling parameters are determined self-consistently by the mean-field parameters. J_v are the spherical components of the angular momentum ($v = \pm 1$). We assume that we are given two static axially symmetric potentials, an isoscalar potential $V_0(r)$ and isovector potential $V_1(r)$, which describe the average nuclear field. According to [58] the isovector part of the nuclear mean field can be written as

$$V_1(r) = \eta \frac{N-Z}{A} \tau_z V_0(r). \quad (7)$$

Here, the parameter $\eta = \frac{V_1}{4V_0}$ and V_0 and V_1 are the isoscalar and isovector depth of the potential wells, respectively.

In the QRPA method, the collective 1^+ states are considered as one-phonon excitations described by

$$|\Psi_i\rangle = Q_i^+|\Psi_0\rangle = \frac{1}{\sqrt{2}} \sum_{ss',\tau} \left[\psi^i_{ss'}(\tau) C^+_{ss'}(\tau) - \varphi^i_{ss'}(\tau) C_{ss'}(\tau)\right]|\Psi_0\rangle, \quad (8)$$

where Q_i^+ is the phonon creation operator, $|\Psi_0\rangle$ is the phonon vacuum which corresponds to the ground state of the even-even nucleus and $C^+_{ss'}$ ($C_{ss'}$) is the two-quasiparticle creation (annihilation) operator. The two-quasiparticle amplitudes $\psi^i_{ss'}$ and $\varphi^i_{ss'}$, are normalized by

$$\sum_{ss'\tau} \left[{\psi^i_{ss'}}^2(\tau) - {\varphi^i_{ss'}}^2(\tau)\right] = 1. \quad (9)$$

Following the well-known procedure of the RPA method, one could find the eigenfunctions and eigenvalues of the Hamiltonian. To obtain the excitation energies, one has to solve the equation of motion

$$\left[H_{sqp} + h_0 + h_1 + V_{\sigma\tau}, Q_i^+\right] = \omega_i Q_i^+. \quad (10)$$

Omitting details of the solution of (10), we give only the most necessary equations. In particular, the secular equation for the excitation energy of 1^+ states can be written as

$$\omega_i^2 J_{eff}(\omega_i) = \omega_i^2 \left[J - 8\chi_{\sigma\tau} \frac{X^2}{D_\sigma} + \frac{\omega_i^2}{\gamma_1 - F_1} \left(J_1^2 - 8\chi_{\sigma\tau} \frac{JX_1^2 - 2J_1 X X_1}{D_\sigma}\right)\right] = 0, \quad (11)$$

and

$$D_\sigma = 1 + \chi_{\sigma\tau} F_\sigma, \qquad X = X_n - X_p,$$
$$\gamma_1 = \gamma_1^n - \gamma_1^p, \qquad J_1 = J_1^n - J_1^p. \quad (12)$$

All the formulae are given clearly in [27]. One of the solutions of eq. (11), with $\omega_0 = 0$, belongs to the rotational excitation state because, as shown [54], it is characterized by definite values of the static electrical and magnetic moments, which coincide with the 2_g^+ state in the generalized model. The static limit of the function $J_{eff}(\omega_0 = 0) = J_\sigma$ determines the moment of inertia of the nucleus and coincides in the form with the well-known expression in the cranking model including the spin-spin forces [59]. The remaining solutions of (11) with $\omega_i > 0$ describe the harmonic vibrations of the system, lying above the threshold of the first two-quasiparticle energy.

3 Magnetic dipole properties of the 1^+ states

Owing to the symmetries of the spin-spin and restoring interactions, and the magnetic dipole operator, the most characteristic value of the 1^+ states is the $M1$ transition probability of the excitation from the ground state, which can be written in the form [27]

$$B\left(M1, 0^+ \to 1_i^+\right) = \frac{3}{4\pi} \left| R_p(\omega_i) + \sum_\tau \left(g_s^\tau - g_l^\tau\right) R_\tau(\omega_i) \right|^2 \mu_N^2, \quad (13)$$

where

$$R_p(\omega_i) = \sum_\mu^{(p)} \varepsilon_\mu j_\mu L_\mu \left(\psi^i_\mu + \varphi^i_\mu\right),$$
$$R_\tau(\omega_i) = \sum_\mu^{(\tau)} \varepsilon_\mu s_\mu L_\mu \left(\psi^i_\mu + \varphi^i_\mu\right).$$

Here ε_μ are two-quasiparticles energies and in the usual notation $L_\mu = u_s v_{s'} - u_{s'} v_s$. The single-particle matrix elements of the spin (s_{+1}) and angular-momentum operator (j_{+1}) are denoted as s_μ and j_μ. g_s and g_l are the spin and orbital gyromagnetic ratios of free nucleons, respectively.

The energy-weighted sum rules [EWSR] for the $M1$ transitions are given as

$$2\sum_i \omega_i B\left(M1, 0^+ \to 1_i^+\right) = \left[\vec{\mu}^+, \left[H, \vec{\mu}\right]\right]_{QRPA}, \quad (14)$$

where

$$\vec{\mu} = g_s^n \vec{s}_n + g_s^p \vec{s}_p + g_l^p \vec{l}_p.$$

Let us calculate the right-hand side of the sum rule in the QRPA

$$\left[\vec{\mu}^+, \left[H, \vec{\mu}\right]\right]_{QRPA} = \frac{3}{4\pi} \left[\gamma_p + \sum_\tau \left(g_s^\tau - g_l^\tau\right)\delta^\tau - \frac{\left(\gamma_p - \gamma_l^p\right)^2}{\gamma - \gamma_1} - \frac{{\gamma_l^p}^2}{\gamma_1}\right] \mu_N^2, \quad (15)$$

where

$$\gamma = \gamma_n + \gamma_p, \qquad \gamma_1 = \gamma_1^n - \gamma_1^p,$$
$$\gamma_\tau = 2\sum_\mu^{(\tau)} \varepsilon_\mu L_\mu^2 j_\mu^2, \qquad \gamma_1^\tau = 2\sum_\mu^{(\tau)} (V_1)_\mu L_\mu^2 j_\mu^2,$$
$$\delta^\tau = 2\sum_\mu^{(\tau)} \varepsilon_\mu L_\mu^2 s_\mu^2.$$

It is important to state that the last two terms in the square brackets of (15) represent the contribution of the effective forces h_0 and h_1 to the sum rule and noticeably affect it.

4 Results and discussion

The numerical calculations have been carried out for a wide range of deformation parameters in the even-even $^{130-136}$Ba isotopes. The single-particle energies are obtained from the Warsaw deformed Woods-Saxon potential [60]. The basis contains all discrete and quasi-discrete levels in the energy region up to 3 MeV. The mean-field deformation parameters δ_2 are calculated according to [61] using deformation parameters β_2 defined from experimental quadrupole moments [40]. The pairing-interaction constants chosen according to Soloviev [62] are based on the single-particle levels corresponding to the nucleus in question. The calculated values of the pairing parameters Δ and λ corresponding to the respective G_N and G_Z and the mean-field deformation parameters δ_2 are shown in table 1. The model contains a single parameter of isovector spin-spin interactions. The spin interaction strength was chosen as $\chi_{\sigma\tau} = 40/A$ MeV [63]. This value allows a satisfactory description of the scissors mode fragmentation in well-deformed rare-earth nuclei (see [27]).

Here we want to study the effect of separation of the spurious rotational states to the properties of the scissors mode 1^+ states. The advantage of separation of the spurious states can be demonstrated by the comparison of the results of the rotational invariant QRPA and the non-rotational invariant one. Distribution of the $M1$ strength for the different RPA solutions ω_i gives important information about the role of effective interactions in the summed $B(M1)$ value of the scissors mode. Distributions of the calculated $B(M1)$ transition strengths in the ^{130,132,134,136}Ba isotopes with respect to 1^+ excitations are represented in fig. 1 and fig. 2.

As seen from the top plots in fig. 1, a considerable consequence of the use of the rotational invariant model (l.h.s. plots of fig. 1) is the redistribution of the 1^+ states and the decreasing of the summed $B(M1)$ values at energies up to 4 MeV in ^{130}Ba. For example, in case of using the Hamiltonian with broken rotational symmetry (r.h.s. plots of fig. 1), the summed $B(M1) = 1.867\mu_N^2$, while in the rotational invariant model, the summed $B(M1) = 1.08\mu_N^2$. In addition, the analysis shows that in the non-rotational invariant model, the spectroscopic 1^+ states are weakly collective. Thus, we see that the models which use the Hamiltonian with broken rotational symmetry strongly overestimate the $M1$ strength at low energy. These results indicate an importance of the models which are free from the low-energy spurious states. It is shown in [64] that taking into account the rotational invariance and separation of the zero energy spurious solutions is important for a correct description of the scissors mode 1^+ states and the ground-state correlations in high versions of the QRPA. The introduction of the restoring forces increases the fragmentation of the scissors mode at low energies and causes collectivization of the states in question. For instance, in ^{132}Ba, apart from the isoscalar forces, the presence of the isovector effective restoring interactions in the Hamiltonian (1) increases the number of 1^+ states and the distribution of the summed $B(M1)$ value at low energy (l.h.s of the bottom plots of fig. 1). Comparing these results with the ones obtained using only the isoscalar restoring forces (r.h.s. of the bottom plot in fig. 1) we observe that, in addition to the isoscalar forces, the consideration of the isovector restoring forces in calculations causes the splitting of the states with large $B(M1)$ strengths and fragments the $M1$ strength into more levels. For example, in the case $h_1 = 0$ the state with energy $\omega = 3.080$ MeV and $B(M1) = 0.182\mu_N^2$ is split into two states with energies $\omega = 3.074$ and $B(M1) = 0.142\mu_N^2$ and $\omega = 3.149$ MeV and $B(M1) = 0.046\mu_N^2$, respectively. Whereas, the most collective orbital state at energy $\omega = 2.844$ MeV with $B(M1) = 0.312\mu_N^2$ is little influenced. Thus, the consideration of the isovector restoring forces in the calculations causes a redistribution of the states and fragments the summed $M1$ strength into more levels. It is important to state that the restoring forces h_0 and h_1 decrease the value of the energy-weighted sum rule for $M1$ transitions in the quasiparticle model of about 15 percent. The sum of the contributions of the three interactions included simultaneously in the Hamiltonian (1) is smaller than the sum of their contributions calculated separately. This fact shows the importance of the interference between these interactions on low-lying 1^+ excitations.

Table 1. Pairing correlation parameters (in MeV) and δ_2 values for the Ba isotopes.

N	Δ_n	λ_n	$G_N A$	Δ_p	λ_p	$G_Z A$	δ_2
74	1.3	−9.091	20.0	1.2	−5.703	23.0	0.171
76	1.3	−8.741	20.0	1.2	−6.283	23.0	0.146
78	1.2	−8.365	20.5	1.1	−6.863	19.5	0.129
80	1.3	−7.891	22.0	1.2	−7.509	21.0	0.106

Now, in the following, we shall discuss ^{134}Ba and compare the calculated results with the experimental data of [33], which are shown in the top plots of fig. 2. In this nucleus theory predicts *many* more low-lying 1^+ states than experiment. There exists one collective state with relatively large $B(M1) = 0.305\mu_N^2$ at energy 2.612 MeV. The orbit-to-spin ratio of the matrix elements of the orbital and spin parts of the $M1$ transition operator for this state is $M_l/M_s = -19$. This state could be identified with the experimentally observed fragment of the scissors mode

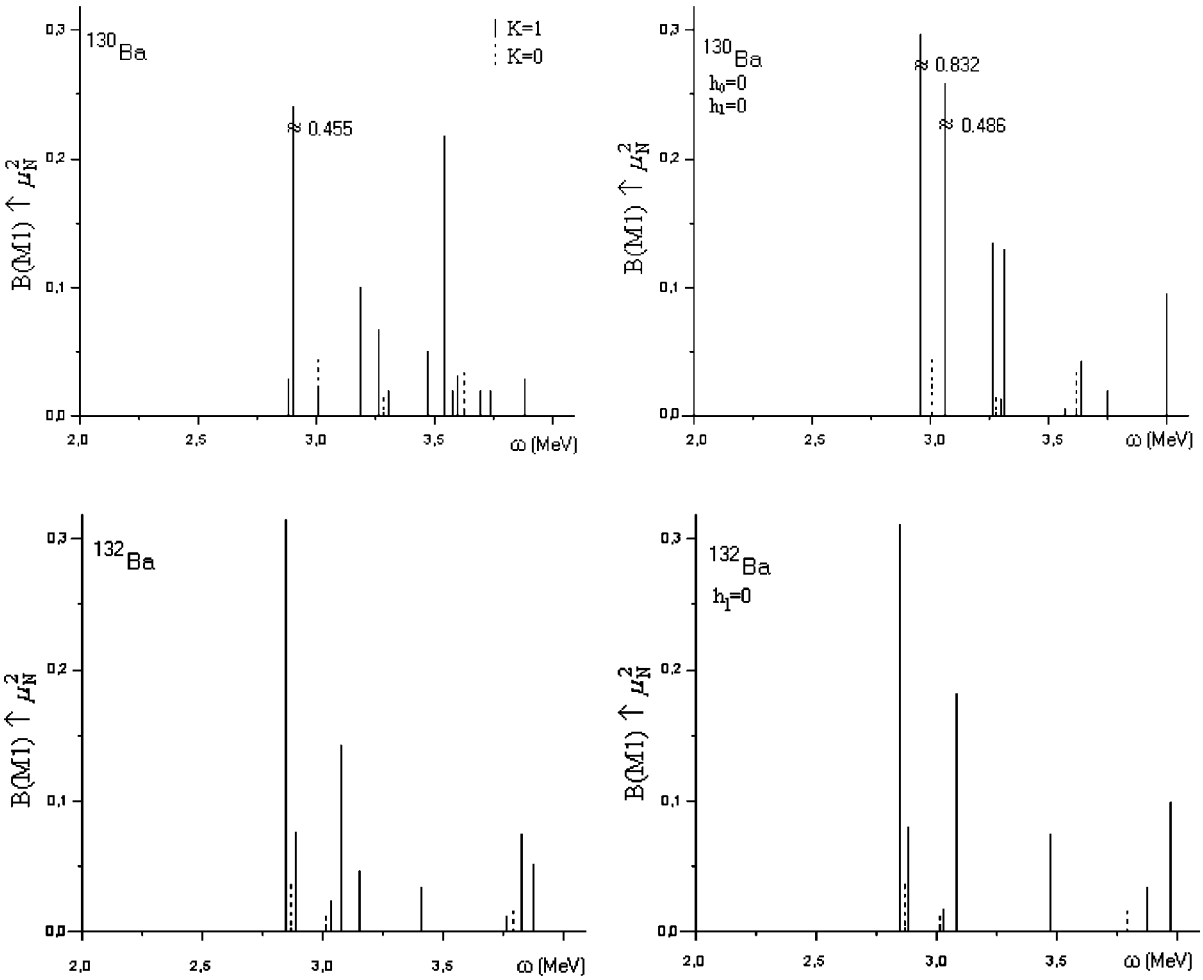

Fig. 1. Energy diagram of $B(M1)$ values calculated for ^{130}Ba and ^{132}Ba isotopes in the QRPA using different approximations for the effective forces. Only states with $B(M1) \geq 0.01\mu_N^2$ are displayed. Detail of the approximation is given in the text.

with $B(M1) = 0.307\mu_N^2$ at 2.939 MeV. Besides, at low-energy the theory indicates the presence of one weakly collectivized spin-vibrational 1^+ state at energy 2.583 with $B(M1) = 0.08\mu_N^2$ for which $M_l/M_s = +5.10^{-2}$. The experimental counterpart of this state could be the state at 2.571 MeV with $B(M1) = 0.08\mu_N^2$ [33].

It is well known that the Gamov-Teller β-decay is selective to the spin contribution of states. Hence, because of the spin character of the state at 2.571 MeV, the β-decay excitation probability should be considerably different (bigger) from the orbital scissors mode state at energy 2.939 MeV. The fact that the $\log ft$ value of the state at 2.571 MeV *is* lower than that of the orbital 1^+ state at 2.939 MeV observed in experiment [65] indicates a larger spin content of the former state than that of the 1^+ state at 2.939 MeV. Therefore, from this comparison and from the decay characteristics of these states, it can be expected that the state at 2.571 MeV observed earlier in β-decay [65] and recently in photon scattering experiment most probably has spin and parity 1^+.

As can be seen from the figures the calculation offers a few weak $M1$ transitions between 3.5 MeV and 4 MeV with summed $B(M1) = 0.10\mu_N^2$. They have a high orbit-to-spin ratio and belong to the scissors mode states which may correspond to some weaker dipole excitations with summed $B(M1) < 0.08\mu_N^2$ clustered at the same energy interval in the experiment.

Comparative characteristics of the low-lying 1^+ excitations of ^{134}Ba, calculated with the non-rotational invariant (1) and the rotational invariant Hamiltonians with the isoscalar (2) and isoscalar plus isovector (3) restoring forces are cited in table 2. Here the excitation energies, $B(M1)$ probabilities and orbit-to-spin ratio are also given.

The calculations show that upon taking into account the rotational invariance the calculated energies are almost similar to each other. Contributions to the summed $B(M1)$ coming from the isoscalar part of the restoring forces are larger than the contributions of the isovector restoring forces. However, the consideration of the isovector restoring forces in the calculations causes a redistribution of the $M1$ strength and influences strongly the orbit-to-spin ratio. The absolute values M_l/M_s fluctuate considerably less in the non-rotational invariant model, although they are also extremely sensitive to the effects of

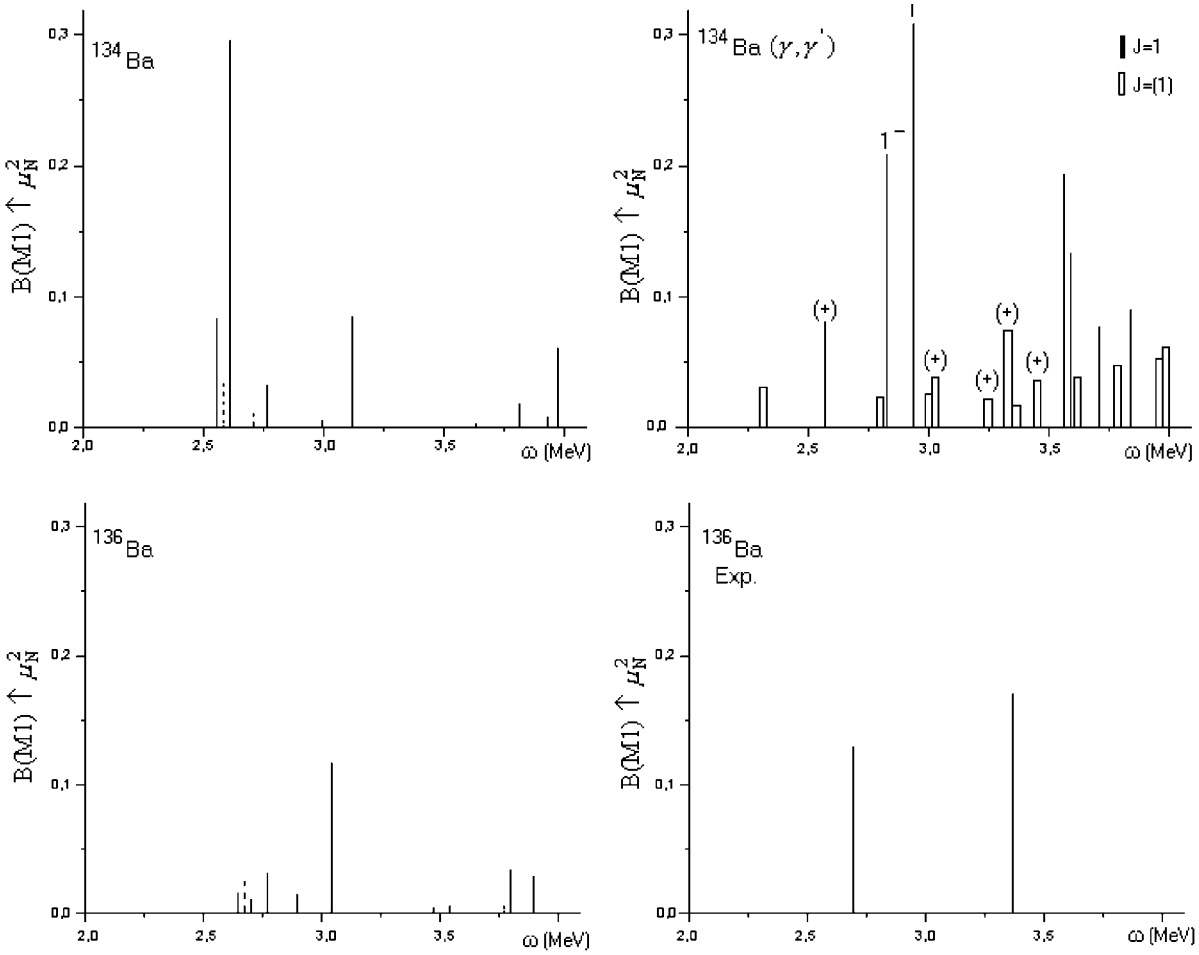

Fig. 2. Comparison of the $B(M1)$ values calculated for the ^{134}Ba and ^{136}Ba nuclei in the rotational invariant QRPA with experimentally observed $M1$ dipole excitations. We present the dipole states with $K = 0$ (dashed line). The NRF experimental data (r.h.s) are taken from [33] for ^{134}Ba and from [34] for ^{136}Ba. Open bars are plotted if $I = 1$ is uncertain. A tentative parity assignment (+) is made if the state is also populated in the β^+-decay of the ground state of ^{134}La. Only states with $B(M1) \geq 0.01\mu_N^2$ are displayed.

Table 2. Comparison of ω_i, $B(M1)$ and M_l/M_s ratio of ^{134}Ba calculated with the non-rotational invariant (1) and rotational invariant Hamiltonians including the isoscalar (2) and isoscalar plus isovector (3) restoring forces. Only states with $B(M1) \geq 0.01\mu_N^2$ are shown.

$H = H_{sqp} + V_{\sigma\tau}$ (1)			$H = H_{sqp} + h_0 + V_{\sigma\tau}$ (2)			$H = H_{sqp} + h_0 + h_1 + V_{\sigma\tau}$ (3)		
ω_i (MeV)	$B(M1)$ μ_N^2	M_l/M_s	ω_i (MeV)	$B(M1)$ μ_N^2	M_l/M_s	ω_i (MeV)	$B(M1)$ μ_N^2	M_l/M_s
2.556	0.72	4.49	2.579	0.14	0.62	2.588	0.08	0.17
2.604	0.22	−4.85	2.603	0.19	−6.3	2.612	0.31	−19
2.615	0.06	−2.64	2.693	0.02	2.2	2.764	0.03	4.5
2.714	0.15	5.18	2.909	0.15	4.6	2.994	0.01	−0.37
2.744	0.10	−4.02	3.236	0.01	1.1	3.119	0.08	$-1.2 \cdot 10^4$
3.240	0.03	4.03	3.805	0.02	3.2	3.810	0.02	2.5
3.785	0.05	4.79	3.916	0.01	19	3.926	0.01	14
–	–	–	3.972	0.06	20	3.972	0.06	18

Table 3. Comparison of $\overline{\omega}$ and summed $B(M1)$ values calculated with the rotational non-invariant (1) and rotational invariant Hamiltonians including the isoscalar (2) and isoscalar plus isovector (3) restoring forces with semi-empirical non–energy-weighted [22] and linear energy-weighted [15] sums with experimentally observed $M1$ dipole excitations (below 4 MeV). The experimental data are taken from [33] for ^{134}Ba and [34] for ^{136}Ba.

Nuclei	$\overline{\omega}$ (MeV)					$\sum_i B(M1,i)$ (μ_N^2)					$\sum_i \omega_i B(M1,i)$ $(\mathrm{MeV}\cdot\mu_N^2)$				
	(1)	(2)	(3)	[22]	exp.	(1)	(2)	(3)	[22]	exp.	(1)	(2)	(3)	[15]	exp.
^{130}Ba	3.21	3.22	3.20	3.96	–	2.15	1.09	1.08	0.92	–	6.90	3.51	3.46	4.28	–
^{132}Ba	3.05	3.15	3.11	3.63	–	1.75	0.81	0.78	0.63	–	5.34	2.55	2.43	2.83	–
^{134}Ba	2.73	2.88	2.88	3.68	3.14	1.59	0.61	0.60	0.50	0.56	4.34	1.76	1.73	2.21	1.76
^{136}Ba	2.81	3.13	3.17	4.96	3.11	1.13	0.25	0.26	0.30	0.26	3.18	0.78	0.82	1.29	0.81

the restoring forces. Note that, in the independent quasiparticle model, the calculation shows that the low-lying (up to energy 4 MeV) two-quasiparticle 1^+ states have mainly orbital character, with the quasiparticles filling the deformed orbitals of the same j-shell near the Fermi surface (subshells $g_{9/2}$ for protons and $h_{11/2}$ for neutrons).

It is instructive to investigate the possible role of the $K = 0$ branch of the 1^+ states at low energy. The theory indicates the presence of two weakly collectivized spin-vibration 1^+ states with $K = 0$ at energy $\omega_1 = 2.588$ MeV with $B(M1) = 0.034\mu_N^2$ and $\omega_2 = 2.711$ MeV with $B(M1) = 0.011\mu_N^2$ in ^{134}Ba. The summed dipole width of these states is 2.3 meV. The contribution of these two states to the total dipole decay width below 4 MeV is smaller than 2%. Thus our results show that in ^{134}Ba all the stronger $M1$ transitions likely have a $\Delta K = 1$ character as in the well-deformed nuclei [9]. Note that this picture is peculiar to all the investigated barium isotopes (see fig. 1 and fig. 2).

The QRPA predictions for the low-energy $M1$ strength distributions in ^{136}Ba and the corresponding experimental data are displayed in the bottom part of fig. 2. While the data show more fragmentation, the total dipole strength is well accounted for. The calculation predicts a few scissors mode 1^+ states up to energy 4 MeV with summed $B(M1) = 0.26\mu_N^2$ and average energy $\overline{\omega} = 3.17$ MeV in accordance with the experimental data [34] of $B(M1) = 0.30\mu_N^2$ with average energy $\overline{\omega} = 3.10$ MeV. The main contribution to the summed $B(M1)$ gives the orbital state at energy 3.043 MeV with transition probability $B(M1) = 0.12\mu_N^2$. The corresponding orbital-to-spin ratio for this state is $M_l/M_s = -13$. Besides, at an energy below 3 MeV theory indicates the presence of a few weekly collectivized spin-vibration 1^+ states with summed $B(M1) = 0.07\mu_N^2$, for which $M_l/M_s \approx -2.10^{-1}$.

The state with orbital character has not been found in the theoretical spectrum of up to 4 MeV in the semimagic nucleus ^{138}Ba ($N = 82$). In NRF experiments [42] no $M1$ excitations could be observed in the magic isotope ^{138}Ba below 4 MeV. In this nucleus the predicted lowest 1^+ states with $B(M1) = 0.12\mu_N^2$ at 4.9 MeV has spin-vibrational character ($M_l/M_s = 10^{-2}$). Similar situations are observed in ^{140}Ce, ^{142}Nd and ^{144}Sm nuclei which also have $N = 82$ neutrons [27,28]. This case shows the importance of the neutron-proton interaction outside of the closed shells in the formation of the scissors mode.

Besides the $B(M1)$ strength another important quantity of the orbital 1^+ states is the average value of the scissors mode excitation energies $\overline{\omega}$. In order to establish the energy centroid of the scissors mode excitations, we use the energy-weighted and non–energy-weighted sum rules of the $M1$ transition matrix elements below 4 MeV,

$$\overline{\omega} = \sum_i \omega_i B(M1,\omega_i) / \sum_i B(M1,\omega_i), \qquad (16)$$

and we are especially interested in the A-dependence of $\overline{\omega}$ and in comparing the experimental data to the theoretical expectations.

The results for the mean energy of the scissors mode excitations, the summed $B(M1)$ and the EWSR, calculated with the rotational non-invariant (1) and rotational invariant Hamiltonians including the isoscalar (2) and isoscalar plus isovector (3) restoring forces, the semi-empirical summed $B(M1)$ [15], the energy-weighted sum rule [22] and the experimentally observed $M1$ dipole excitations are given in table 3.

The results of the calculations show that the rotational non-invariant model (1) exceeds the experimental values of the $B(M1)$ more than two times. Indeed, the introduction of the restoring forces (3) essentially reduces the $B(M1)$ strength and decreases substantially the discrepancy with the experiments. As can be seen from table 3 the predicted semi-empirical values of the summed $M1$ strengths [22] are close to the measured values for ^{134}Ba and ^{136}Ba. However, the mean excitation energies of the scissors mode calculated in this model are larger than the ones deduced from the experiment. On the other hand, the semi-empirical results of the EWSR [15] overestimate the experimental data by almost a factor of 1.5. Thus, we see that the models which use the Hamiltonian with broken symmetry strongly overestimate the summed $M1$ strength at low energies.

5 Conclusions and outlook

In this paper, the QRPA approach suggested in [27] has been carried out to describe $K^\pi = 1^+$ states in the even-even $^{130-136}$Ba nuclei. The effects of the separation of the spurious state on the properties of scissors mode excitations have been investigated. The marked differences be-

tween the results for 1^+ states, calculated with and without taking into account the rotational invariance indicate the importance of the approaches which are free from spurious low-energy solutions. A separation of the rotational state from the 1^+ states changes somewhat the distribution of the $B(M1)$ strength in the spectroscopic energy region and increases the fragmentation of the scissors mode 1^+ excitations in agreement with the experimental data. Similarly to well-deformed nuclei low-lying $M1$ transitions mainly have $\Delta K = 1$ character for all the nuclei under investigation. The relative contribution of $\Delta K = 0$ transitions to the total dipole decay width below 4 MeV is smaller than 2% for all nuclei under investigation and the $M1$ strength is usually smeared out over the entire energy interval between 2 and 4 MeV with little or no clustering. The mixing of the scissors mode states with the spin-vibrational 1^+ states is poor due to the different selection rules of the matrix elements of the orbital and spin operators. The destructive interference between the orbit and spin parts of the $M1$ strength has been found for the ^{134}Ba and ^{136}Ba isotopes near the shell closer closure.

Consideration of isovector restoring forces in the calculations causes the splitting of the states with large $B(M1)$ strengths and fragments the $M1$ strength into more levels. The choice of the isoscalar and isovector forces in a self-consistent manner with mean-field potentials based on the rotational invariance of the Hamiltonian makes it possible to treat the scissors mode more rigorously without any extra quadrupole-quadrupole interaction parameter which is different in the case of the β- and γ-vibrations. Obviously, more experimental data with good accuracy are needed to obtain detailed information on the signature of the scissors mode $M1$ states and to draw a decisive conclusion in transition nuclei.

We are very much indebted to referees for helpful remarks on an earlier version of the manuscript and Prof. Giuseppina Orlandini for his tolerance and patience. We wish to express our thanks to Dr. M. Bektasoglu for his most careful reading of the manuscript and useful comments. A. Guliyev acknowledges support from the TÜBITAK, Turkey.

References

1. A. Richter, Prog. Part. Nucl. Phys. **34**, 261 (1995).
2. N. Lo Iudice, F. Palumbo, Phys. Rev. Lett. **41**, 1532 (1978).
3. F. Iachello, Nucl. Phys. A **358**, 89c (1981).
4. D. Bohle *et al.*, Phys. Lett. B **137**, 27 (1984).
5. U. Kneissl *et al.*, Prog. Part. Nucl. Phys. **37**, 349 (1996).
6. W. Ziegler *et al.*, Phys. Rev. Lett. **65**, 2515 (1990).
7. J. Margraf *et al.*, Phys. Rev. C **47**, 1474 (1993).
8. P. von Neumann-Cosel *et al.*, Phys. Rev. Lett. **75**, 4178 (1995).
9. A. Zilges *et al.*, Nucl. Phys. A **599**, 147c (1996); A. Zilges *et al.*, Phys. Rev. C **42**, 1945 (1990).
10. T. Suzuki, D. Rowe, Nucl. Phys. A **289**, 461 (1977).
11. E. Lipparini, S. Stringari, Phys. Lett. B **130**, 139 (1983).
12. D. Bes, R. Broglia, Phys. Lett. B **137**, 141 (1984).
13. R. Hilton, Z. Phys. A **316**, 121 (1984).
14. A. Nojarov *et al.*, Nucl. Phys. A **563**, 349 (1994); Phys. Rev. C **41**, 1243 (1990); Nucl. Phys. A **492**, 105 (1989); **484**, 1 (1988).
15. E. Moya De Guerra, L. Zamick, Phys. Rev. C **47** 2604 (1993); A.Y.L. Diepernik, E. Moya De Guerra, Phys. Lett. B **189**, 267 (1987); **196**, 409 (1987).
16. J. Speth, D. Zawischa, Phys. Lett. B **211**, 247 (1988).
17. A.A. Raduta, N. Lo Iudice, I.I. Irsu, Nucl. Phys. A **584**, 84 (1995).
18. V.G. Soloviev *et al.*, Nucl. Phys. A **600**, 155 (1996).
19. N. Lo Iudice, A. Richter, Phys. Lett. B **304**, 193 (1993).
20. N. Lo Iudice, A. Raduta, D. Delion, Phys. Rev. C **50**, 127 (1994).
21. J. Enders *et al.*, Phys. Rev. C **59**, R1851 (1999).
22. J. Enders *et al.*, Phys. Rev. C **71**, 014306 (2005).
23. I. Hamamoto, C. Magnusson, Phys. Lett. **260**, 6 (1991).
24. K. Heyde, C. De Coster, Phys. Rev. C **44**, R2262 (1991).
25. E. Garrido *et al.*, Phys. Rev. C **44**, R2150 (1991).
26. P. Sarriguren *et al.*, J. Phys. G **20**, 315 (1994); Phys. Rev. C **54**, 690 (1996).
27. A.A. Kuliev *et al.*, Int. J. Mod. Phys. E **9**, 249 (2000).
28. A.A. Kuliev *et al.*, J. Phys. G **28**, 407 (2002).
29. D. Zawischa, J. Phys. G **24**, 683 (1998).
30. N. Lo Iudice, Riv. Nuovo Cimento **23**, 1 (2000).
31. P. von Brentano *et al.*, Phys. Rev. Lett. **76**, 2029 (1996).
32. A. Linnemann *et al.*, Phys. Lett. B **554**, 15 (2003).
33. H. Maser *et al.*, Phys. Rev. C **54**, R2129 (1996).
34. N. Pietralla *et al.*, Phys. Rev. C **58**, 796 (1998).
35. C. Fransen *et al.*, Phys. Rev. C **59**, 2264 (1999).
36. R. Georgii *et al.*, Phys. Lett. B **351**, 82 (1995).
37. R. Schwengner *et al.*, Nucl. Phys. A **620**, 277 (1997).
38. N. Pietralla *et al.*, Phys. Rev. Lett. **83**, 1303 (1999).
39. N. Pietralla *et al.*, Phys. Rev. C **58**, 191 (1998).
40. S. Raman *et al.*, At. Data Nucl. Data Tables **36**, 1 (1987); **78**, 1 (2001).
41. P. Petkov *et al.*, Phys. Rev. C **51**, 2511 (1995).
42. M. Scheck *et al.*, Phys. Rev. C **70**, 044319 (2004).
43. H. Harter *et al.*, Phys. Lett. B **205**, 174 (1988).
44. E. Hammaren *et al.*, Phys. Lett. B **171**, 347 (1986).
45. A. Nowoselsky, I. Talmi, Phys. Lett. B **172**, 139 (1986).
46. G. Puddi, O. Scholten, T. Otsuka, Nucl. Phys. A **348**, 109 (1988).
47. E. Guliyev *et al.*, Bulg. J. Phys. **27**, 17 (2000).
48. E. Guliyev *et al.*, Nucl. Phys. A **690**, 255c (2001).
49. V.Yu Ponomarev *et al.*, Phys. Lett. B **97**, 4 (1980).
50. E. Guliyev *et al.*, Phys. Lett. B **532**, 173 (2002).
51. N. Pyatov, M. Cherney, Sov. J. Nucl. Phys. **16**, 931 (1972).
52. N. Pyatov, D. Salamov, Nucleonica **22**, 127 (1977).
53. K.G. Dietrich *et al.*, Phys. Lett. B **220**, 351 (1985).
54. N. Lo Iudice, Nucl. Phys. A **605**, 61 (1996).
55. P. Magierski, R. Wyss, Phys. Lett. **486**, 54 (2000).
56. A.A. Kuliev, N. Pyatov, Sov. J. Nucl. Phys. **20**, 297 (1974).
57. I. Hamamoto, W. Nazarewicz, Phys. Lett. B **297**, 25 (1992).
58. O. Bohr, B. Mottelson, *Nuclear Structure*, Vol. **1** (Benjamin, New York Amsterdam, 1969).
59. O. Prior *et al.*, Nucl. Phys. A **110**, 257 (1968).
60. J. Dudek, T. Werner, J. Phys. G **4**, 1543 (1978).
61. O. Bohr, B. Mottelson, *Nuclear Structure*, Vol. **2** (Benjamin, New York Amsterdam, 1975).
62. V.G. Soloviev, *Theory of Complex Nuclei* (Pergamon Press, New York, 1976).
63. S. Gabrakov *et al.*, Nucl. Phys. A **182**, 625 (1972).
64. A.A. Kuliev *et al.*, J. Phys. G **30**, 1253 (2004).
65. R.C. Greenwood *et al.*, Phys. Rev. C **14**, 1906 (1976).